



CHALMERS
UNIVERSITY OF TECHNOLOGY

IMPACT OF PROCESSING PARAMETERS ON THE MULTIFUNCTIONALITY OF CARBON FIBRES FOR STRUCTURAL

Downloaded from: <https://research.chalmers.se>, 2024-07-17 11:23 UTC

Citation for the original published paper (version of record):

Tavano, R., Xu, J., Liu, F. et al (2024). IMPACT OF PROCESSING PARAMETERS ON THE
MULTIFUNCTIONALITY OF CARBON FIBRES FOR STRUCTURAL
BATTERY ELECTRODES. Proceedings of the 21st European Conference on Composite Materials,
6: 224-231. <http://dx.doi.org/10.60691/yj56-np80>

N.B. When citing this work, cite the original published paper.

IMPACT OF PROCESSING PARAMETERS ON THE MULTIFUNCTIONALITY OF CARBON FIBRES FOR STRUCTURAL BATTERY ELECTRODES

Ruben Tavano^{1*}, Johanna Xu¹, Fang Liu¹, Claudia Creighton², Bhagya Dharmasiri², Luke C. Henderson², Leif E. Asp¹

¹Industrial and Materials Science, Chalmers University of Technology, 41258 Göteborg, Sweden

²Institute of Frontier Materials, Deakin University, Geelong Waurn Ponds Campus, VIC 3216, Australia

* Corresponding author (ruben.tavano@chalmers.se)

Keywords: *Carbon fibre, Structural batteries, Multifunctionality*

Abstract

Carbon fibres are multifunctional materials considered for the realisation of structural battery electrodes. Processing conditions affect the carbonaceous microstructure of carbon fibres. The microstructure dictates the fibre's mechanical properties, i.e. modulus and strength, as well as its electrochemical capacity. Here, carbon fibre processing conditions are investigated to identify the effect of applied tension during the stabilisation step and carbonisation temperature on carbon fibre multifunctionality. First, different pulling forces are employed during the stabilisation step. The most promising carbon fibre resulting from changing the applied force is then subjected to varying temperatures in the carbonisation step. The precursor material and the oxidation temperatures are kept constant. The carbonaceous microstructure of fibres is investigated via wide-angle X-ray scattering (WAXS) and transmission electron microscopy (TEM) analyses to determine the effect of different processing parameters. Mechanical and electrochemical tests are performed to characterise carbon fibre multifunctionality with respect to mechanical and electrochemical performance. A moderate trade-off between mechanical and electrochemical performance is demonstrated, where the elastic modulus and strength decrease and the electrochemical capacity increases with reduced tensions and carbonisation temperature. Thus, fibres customised for targeted multifunctionality within a limited design space can be realised by carefully selecting the processing conditions in conventional carbon fibre manufacture.

1. Introduction

Multifunctional materials have the potential to change the field of energy storage in transportation. Efficiency is a key aspect of electric mobility and this can be greatly improved if we use multifunctional systems such as structural battery composites (SBC). In these devices, electrical energy storage can be integrated into structural components, thus the structural battery composite can simultaneously store electric energy and carry mechanical loads. Common configurations for structural batteries consist of a carbon fibre negative electrode, and a counter electrode, divided by a glass fibre separator. All the layers are then infused with a structural battery electrolyte (SBE). Here, the carbon fibres are the crucial multifunctional constituent, acting as the host for lithium ions, electron conductors, and reinforcement^{[1]-[6]}.

The potential for carbon fibres to be used as a lithium-ion storage medium, similarly to what was done with graphite particles, was recognized in the early 1990s by Ruland^[7]. A few years later, Snyder et al. showed that polyacrylonitrile (PAN)-based carbon fibres can guarantee higher capacities than pitch-based carbon fibres, making them more suitable for this type of application^[8]. Historically, commercial carbon fibres have been designed with mechanical properties in mind. For this reason, the relation between these and the different microstructures which could be achieved by changing the processing

parameters was well understood^{[9][10]}. However, the relationship between the electro-chemo-mechanical performance of the fibre and its microstructure is yet not well understood.

Recent works in the structural battery composite community have looked at how lithium ions entering the carbon fibres affect the physical and mechanical properties of carbon fibres^{[11]–[14]}, and in further studies, the electrochemical performance of widely used commercially available PAN-based carbon fibres was characterised^{[15],[16]}. Better electrochemical capacity was observed for intermediate modulus (IM) carbon fibres, compared to high modulus (HM) carbon fibres, but the reasons behind the different performance were unknown. Fredi et al. studied the lithiation mechanism for common IM and HM carbon fibres using high-resolution transmission electron microscopy (TEM) and in situ Raman spectroscopy^[17]. They found that IM carbon fibres insert lithium with a mechanism similar to amorphous carbon. In contrast, HM carbon fibres inserted lithium with a staging mechanism closer to that observed in graphite. HM carbon fibres showed a lower electrochemical capacity compared to IM carbon fibres. This difference was explained by considering that the staging process was partly hindered by defects present in the large crystallites of the turbostratic graphitic structure observed in HM carbon fibres. A difference in performance between different IM carbon fibres was also observed. This was partially explained by Johansen et al. by considering the differences in the residual amount and type of heteroatoms found in the microstructure^[18]. They found that the nitrogen heteroatom configuration can change among IM carbon fibres. For the two carbon fibres considered, IMS65 carbon fibres showed a larger proportion of pyridinic and pyrrolic nitrogen (20.5%), compared to the 14.2% found for T800 carbon fibres. In this case, pyridinic and pyrrolic nitrogen atoms are close to defect-rich areas of the carbonaceous structure, where lithium ions can be stored in larger amounts. The higher amounts of pyridinic and pyrrolic nitrogen, hence, offer a plausible explanation for the difference in capacity found for IMS65 and T800 fibres^[18]. The mechanism of lithium insertion in the carbon fibres was further studied by Johansen et al. They showed that lithium ions distribute uniformly within the carbon fibres and that a significant part of the first cycle losses measured for carbon fibres is related to lithium ions being trapped in the carbon fibre microstructure^{[19][20]}.

To take advantage of the potential of IM carbon fibres, Asp et al. employed T800 carbon fibres as the negative electrode in a laminated structural battery composite^[21]. They reported a structural battery composite cell with an energy density of 24 Wh kg⁻¹ and an elastic modulus of 25 GPa. Furthermore, Xu et al. realised a multicell structural battery laminate by connecting three of these cells in series, indicating that larger multifunctional systems can be realised^[22]. Finally, improvements in the manufacturing process were proposed by Siraj et al.^[23]. They significantly improved the performance and the repeatability of the cells by using a vacuum-assisted infusion process for the SBE. An energy density of 41.2 Wh kg⁻¹ was reported.

Commercial carbon fibres are not designed with multifunctionality in mind. Additionally, their use in multifunctional applications is complicated due to lack of information about the manufacturing process and the applied sizing. To address these limitations, we studied how the manufacturing process affects the microstructure and subsequently the multifunctionality, in an effort to improve the performance of structural battery composites. This has been done in two consecutive studies.

In the first study, Xu et al. considered different applied tensions during the stabilisation stage, with three different fibre types manufactured using low tension (LT), medium tension (MT) and high tension (HT)^[24]. In this study, every parameter was kept unchanged apart from the tension during the stabilisation stage.

Starting from the previous work by Xu et al., in the second study, the effect of the carbonisation temperature was investigated. Three different types of carbon fibres were manufactured by considering three temperature profiles for the low-temperature (LT) and high-temperature (HT) carbonisation ovens^[25]. In this study, every parameter was kept unchanged and identical to the MT trial from the previous study. The only differences were in the carbonisation temperature profiles used. Three carbon fibre types were manufactured and studied. These were made using a cool temperature profile (CP), an intermediate temperature profile (IP), and a warm temperature profile (WP). Analyzing the manufactured carbon fibres offers deeper insights into how the tension applied during stabilization and

the temperatures utilized in the carbonization process impact the multifunctional capabilities of these fibres. Gaining a comprehensive understanding of how pulling tension and carbonization temperature influence the mechanical and electrochemical properties of carbon fibres holds the promise of realizing structural battery composites with markedly enhanced multifunctional performance.

2. Methods

2.1. Materials

Carbon fibres were manufactured at the Carbon Nexus facilities, Institute for Frontier Materials, Deakin University (Australia) on an advanced research line. A schematic of the manufacturing line is shown in Figure 1.

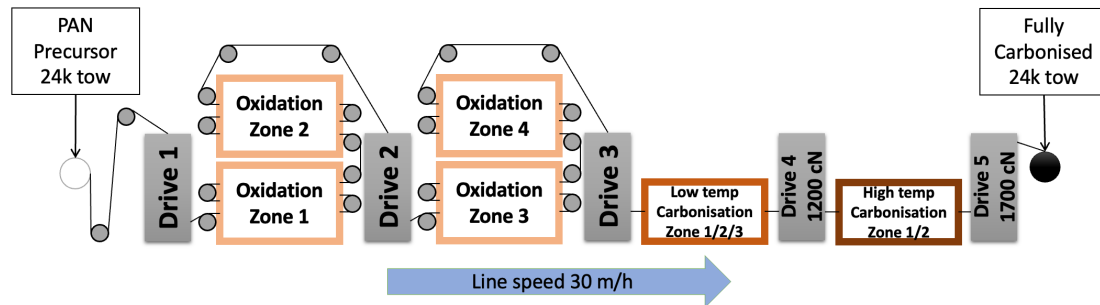


Figure 1. Schematic of the manufacturing process and the used research line.

24 K tows of polyacrylonitrile (PAN) fibres were used as the precursor. These precursor fibres were subjected to a stabilisation process in 4-zone oxidation ovens at temperatures between 228 °C and 258 °C.

For the first study, an average tension was applied to the tow during stabilisation (drive 1, drive 2, and drive 3 in Figure 1), ranging from 720 cN for the low tension (LT) trial, to 2300 cN for the medium tension (MT) trial, to 3025 cN for the high tension (HT) trial. These tensions are representative of the minimum and maximum tensions which could be achieved without breaking the fibre tow. Furthermore, temperatures between 400 °C and 900 °C in the low-temperature carbonisation step and between 1200 °C and 1400 °C in the high-temperature carbonisation step were used.

For the second study, the same tension of 2300 cN as in MT fibres was applied during the stabilisation process. The considered precursor fibres and the oxidation temperatures were kept unchanged from the previous study. Three different temperature profiles were considered for the carbonisation steps. The trials have been named cool profile (CP) for the lower temperature profile, intermediate profile (IP) for the medium temperature profile, and warm profile (WP) for the higher temperature profile. The tension applied at the low temperature and high-temperature carbonization for all fibre types was set to 1200 cN and 1700 cN, respectively. Overall, a line speed of 30 m/h was achieved. A summary of the process parameters used in the two studies is presented in Table 1.

Table 1. Tensions and carbonization temperatures used in the different trials of the two studies (yellow background for the first study and blue background for the second study).

Carbon fibre type	Applied tension in stabilization [cN]	Temperatures in low-temperature carbonization ovens Z1/Z2/Z3 [°C]	Temperatures in high-temperature carbonization ovens Z1/Z2 [°C]
LT	720	400/650/900	1200/1400
MT	2300	400/650/900	1200/1400
HT	3025	400/650/900	1200/1400
CP	2300	284/450/600	1000/1300
IP	2300	350/550/700	1100/1400

WP	2300	450/650/800	1200/1500
----	------	-------------	-----------

2.1. Characterisation techniques

The fibres were characterised using different techniques to determine physical, mechanical, electrochemical, and microstructural properties.

The fibre diameter was measured by using a CottonscopeHD instrument employing laser imaging so that an average value of diameter could be obtained.

The density of the carbon fibres was measured using a density gradient column by ASTM D1505-10.

The surface area was measured by Brunauer-Emmett-Teller (BET) surface area analysis using an inverse gas chromatography surface energy analyser, iGC-SEA employing octane as the adsorbed gas. The surface of the carbon fibres was also investigated using a scanning electron microscope LEO-1550.

WAXS measurements were performed at the Australian Synchrotron beamline and at the Institute for Frontier Materials, Deakin University. The obtained scattering patterns along the equatorial direction were transformed into a series of X–Y plots with the scattering angle (q) plotted against the X-ray intensity using an integration along the equatorial direction, with an azimuthal angle of $\pm 2^\circ$. The peaks were then fitted using a pseudo-Voigt function^[26]. The full width at half maximum (FWHM) of the fitted curve's peak was used to determine the crystallite height L_c , using Scherrer's equation^[27], while the peak position was used to determine the d-spacing of the lattice according to Bragg's law^[28].

TEM was used to investigate the microstructure of the manufactured carbon fibres. Thin lamellae samples with 100 nm thicknesses were prepared using a focused ion beam and scanning electron microscope (FIB/SEM) with an in-situ lift-out technique. A Versa 3D DualBeam FIB/SEM instrument equipped with a gallium ion source for ion milling, an injection system for platinum deposition, and a micro-manipulation system was used. A FEI Titan 80-300 TEM with an accelerating voltage of 300 kV was later used on the thin lamellae to investigate the microstructure of the carbon fibres.

The elastic modulus, tensile strength and strain to failure were measured using a single fibre tensile tester Favimat+ (Textechno, Germany). A 210 cN load cell, a gauge length of 20 mm, and a pulling speed of 1 mm/min were used.

Electrochemical testing was performed using two-electrode pouch cells. Copper strip current collectors were attached to the carbon fibre tows using silver paint. The samples were dried at 50 °C in vacuum overnight before being assembled in an argon-filled glove box. A lithium metal foil acted as the counter and reference electrode, and a 260 mm thick glass fibre layer (Whatman GF/A) acted as the separator. A solution of 1.0 M lithium hexafluorophosphate (LiPF₆) in ethylene carbonate and diethyl carbonate (EC:DEC) (1:1 by weight) was used as the electrolyte in the first study. A 1.0 M lithium bis(trifluoromethanesulfonyl)imide (LiTFSI) salt in a 1:1 by weight mixture of ethylene carbonate and propylene carbonate (EC:PC) was used as the electrolyte in the second study. Galvanostatic charge/discharge cycling was performed to obtain the specific capacity, first cycle losses, and coulombic efficiencies of the carbon fibre electrodes. The electrochemical cycling was done using a Neware CT-4008-5V10mA-164 battery cycler. The half-cells were cycled between 0.01 V and 1.50 V vs Li/Li⁺, and the currents used corresponded to current densities of 0.1C, 0.2C, and 0.4C, based on graphite's theoretical maximum capacity of 372 mAh g⁻¹. The cycling sequence consisted of ten cycles at 0.1C, five cycles at 0.2C, five cycles at 0.4C, and five cycles at 0.1C.

3. Results and conclusion

In these studies, the relation between the microstructure and the mechanical and electrochemical performance has been studied by looking at how different tensions applied during the stabilisation step and different carbonisation temperatures affect the multifunctionality of carbon fibres.

The physical properties of all six fibre types are reported in Table 2. Similar densities are obtained for all the fibres, while for the fibre diameter and the surface area, a stronger effect of the applied tension during the stabilisation step can be seen compared to the carbonisation temperature.

Table 2. Physical properties for the manufactured carbon fibres (yellow background for the first study and blue background for the second study).

Carbon fibre type	Fibre diameter [μm]	Density [g cm^{-3}]	Surface area [$\text{m}^2 \text{g}^{-1}$]
LT	8.42	1.735	0.61
MT	7.32	1.750	0.71
HT	6.89	1.771	0.75
CP	7.50	1.793	1.17
IP	7.71	1.783	0.96
WP	7.82	1.786	1.13

The microstructure determined via WAXS showed that the crystallite height increases with the application of higher tension during the stabilization process as well as with an increased carbonisation temperature. The opposite is true for the d-spacing which is decreased with an increase of the applied tension during the stabilisation and the carbonisation temperatures. The results are shown in Table 3.

Table 3. Microstructural features obtained from WAXS analyses (yellow background for the first study and blue background for the second study).

Carbon fibre type	Crystallite height L_c [nm]	d-spacing [\AA]
LT	1.60	3.51
MT	1.63	3.50
HT	1.69	3.49
CP	1.62	3.55
IP	1.72	3.50
WP	1.77	3.44

The TEM micrographs showed that the LT and MT fibres, and the fibres from the second study, share many similarities in terms of microstructure. Similar crystallite sizes are observed and a uniform distribution of amorphous and crystalline domains is clearly distinguishable. HT fibres on the other hand show a more crystalline microstructure. The TEM micrographs for all the fibres are shown in Figure 2.

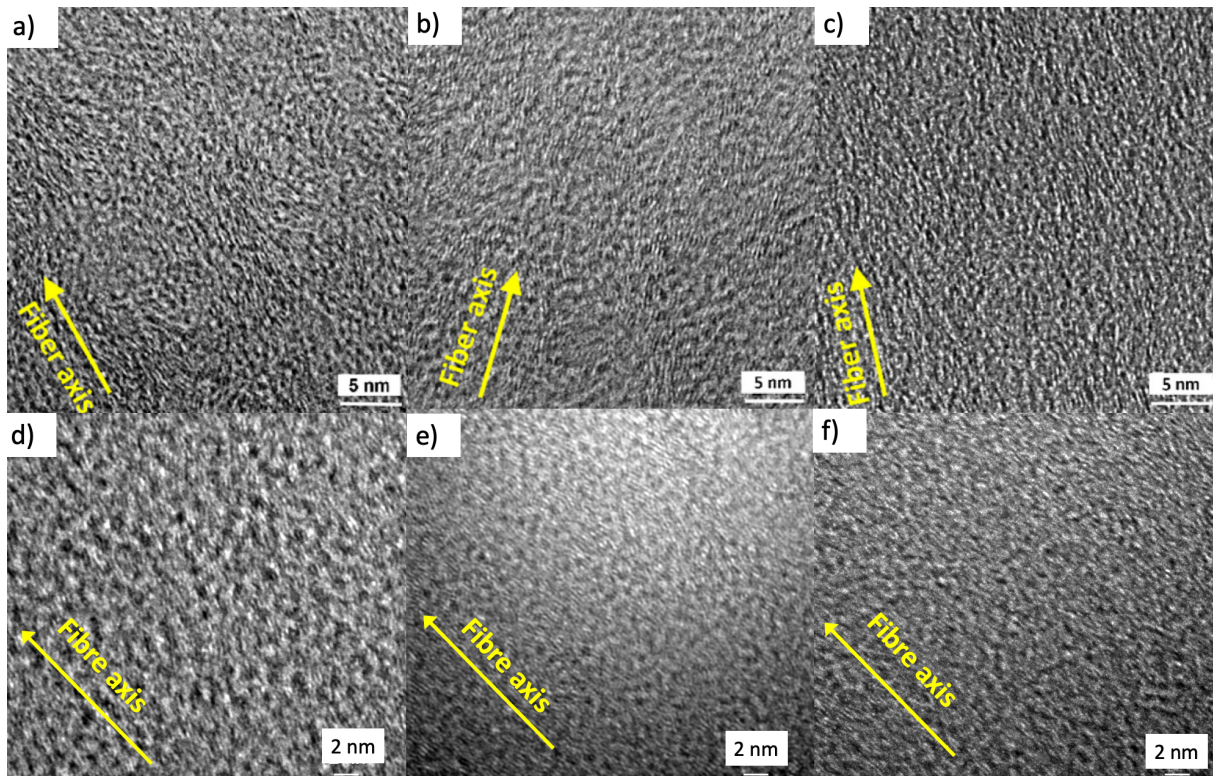


Figure 2. TEM micrographs of the manufactured carbon fibres. (a) Low tension (LT), (b) medium tension (MT), (c) high tension (HT)^[24], (d) cool profile (CP), (e) intermediate profile (IP), (f) warm profile (WP)^[25].

A trade-off was found for the multifunctionality. In the first study, the mechanical properties were increased when the applied tension during the stabilisation step was increased, but at the same time, the electrochemical capacity was decreased. This is due to a stronger alignment of the crystalline domains along the fibre longitudinal direction^[29] and an increase in the crystallite size¹⁷. An identical trend was found when changing the carbonisation temperature, with improved mechanical properties with higher carbonisation temperatures, but lower electrochemical performance. In this case, the trade-off is smaller and the main cause of the difference is the increase in crystallite size which is accompanied by a smaller d-spacing.

In all cases, good coulombic efficiencies above 99% were achieved, as well as good reversibility of lithiation and delithiation capacities for different C-rates. Furthermore, the fibres manufactured in the first study showed higher capacities than those manufactured in the second study. However, due to the time passed between the two studies, some differences in the conditions of the PAN-based precursors, in the composition of the used electrolyte, and possible dissimilarities in the manual assembly process of the half-cells, could partly explain the variance of results.

The changes in multifunctional performance are related to differences in the achieved graphitic microstructure, which could be observed with the WAXS and TEM analyses. These studies reveal that both crystalline and amorphous phases affect the electrochemical performance, as high capacity is achieved by having smaller crystallites and higher d-spacing. Compared to the previously studied commercially available carbon fibres, the capacity was improved in all the manufactured fibres but the mechanical properties were lower for all the fibres. Only in MT and HT fibres, a similar elastic modulus was achieved but a significantly lower tensile strength was also obtained. Overall, this shows that the MT carbon fibre is the most promising one. A summary of the results is shown in Figure 3.

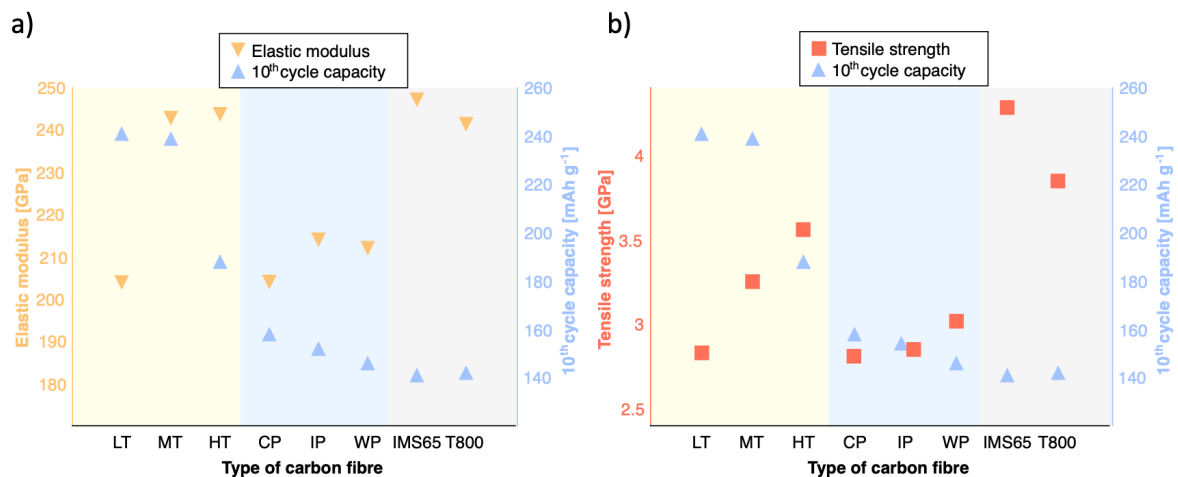


Figure 3. Multifunctionality comparison for (a) elastic modulus and (b) tensile strength compared to 10th cycle capacity (Fibres from the first study with yellow background, fibres from the second study with blue background, commercially available fibres with grey background).

The results of the two studies indicate that for PAN-based carbon fibres with properties similar to those of IM carbon fibres, the design window is narrow. To significantly expand the design possibilities for multifunctional carbon fibres, a much broader processing window in carbon fibre manufacturing will be necessary.

Acknowledgments

The authors would like to thank the following entities for funding this research: United States Air Force (USAF), USA, Award Number FA8655-21-1-7038, Office of Naval Research (ONR), USA, Award Numbers N62909-22-1-2037 and N62909-22-1-2052, Swedish National Space Agency, Contract 2020-00256, Swedish Energy Agency, Contract 46598-1, 2D TECH VINNOVA Competence Center, Contract 2019-00068. This work was partly performed at the Chalmers Material Analysis Laboratory (CMAL).

References

- [1] L.E. Asp, E.S. Greenhalgh, *Compos. Sci. Technol.* **2014**, *101*, 41.
- [2] L.E. Asp, M. Johansson, G. Lindbergh, J. Xu, D. Zenkert, *Funct. Compos. Struct.* **2019**, *1*, 042001.
- [3] T. Jin, G. Singer, K. Liang, Y. Yang, *Mater Today* **2023**, *62*, 151.
- [4] W. Johannisson, D. Zenkert, G. Lindbergh, *Multifunct. Mater.* **2019**, *2*, 035002.
- [5] C. Meng, N. Muralidharan, E. Teblum, K.E. Moyer, G.D. Nessim, C.L. Pint, *Nano Lett.* **2018**, *18*, 7761.
- [6] K. Moyer, C. Meng, B. Marshall, O. Assal, J. Eaves, D. Perez, R. Karkkainen, L. Roberson, C.L. Pint, *Energy Storage Mater* **2020**, *24*, 676.
- [7] W. Ruland, *Adv. Mater.* **1990**, *2*, 528.
- [8] J.F. Snyder, E.L. Wong, C.W. Hubbard, *J. Electrochem. Soc.* **2009**, *156*, A215.
- [9] S.-J. Park, in *Carbon Fibers* (Ed: S.-J. Park), Springer, Singapore **2018**, 31.
- [10] D.J. Johnson, *J. Phys. D: Appl. Phys.* **1987**, *20*, 286.
- [11] E. Jacques, M. H. Kjell, D. Zenkert, G. Lindbergh, *Carbon* **2014**, *68*, 725.
- [12] E. Jacques, M. Hellqvist Kjell, D. Zenkert, G. Lindbergh, M. Behm, *Carbon* **2013**, *59*, 246.
- [13] E. Jacques, M.H. Kjell, D. Zenkert, G. Lindbergh, M. Behm, M. Willgert, *Compos Sci Technol* **2012**, *72*, 792.
- [14] S. Duan, A.H.S. Iyer, D. Carlstedt, F. Rittweger, A. Sharits, C. Maddox, K.-R. Riemschneider, D. Mollenhauer, M. Colliander, F. Liu, L.E. Asp, *Carbon* **2021**, *185*, 234.
- [15] M.H. Kjell, E. Jacques, D. Zenkert, M. Behm, G. Lindbergh, *J. Electrochem. Soc.* **2011**, *158*, A1455.

- [16] J. Hagberg, S. Leijonmarck, G. Lindbergh, *J. Electrochem. Soc.* **2016**, *163*, A1790.
- [17] G. Fredi, S. Jeschke, A. Boulaoued, J. Wallenstein, M. Rashidi, F. Liu, R. Harnden, D. Zenkert, J. Hagberg, G. Lindbergh, P. Johansson, L. Stievano, L.E. Asp, *Multifunct. Mater.* **2018**, *1*, 015003.
- [18] M. Johansen, C. Schlueter, P.L. Tam, L.E. Asp, F. Liu, *Carbon* **2021**, *179*, 20.
- [19] M. Johansen, J. Xu, P.L. Tam, L.E. Asp, F. Liu, *Applied Surface Science* **2023**, *627*, 157323.
- [20] M. Johansen, M.P. Singh, J. Xu, L.E. Asp, B. Gault, F. Liu, *Carbon* **2024**, 119091.
- [21] L.E. Asp, K. Bouton, D. Carlstedt, S. Duan, R. Harnden, W. Johannisson, M. Johansen, M.K.G. Johannisson, G. Lindbergh, F. Liu, K. Peuvot, L.M. Schneider, J. Xu, D. Zenkert, *Adv Energy Sustain Res* **2021**, *2*, 2000093.
- [22] J. Xu, Z. Geng, M. Johansen, D. Carlstedt, S. Duan, T. Thiringer, F. Liu, L.E. Asp, *EcoMat* **2022**, *4*.
- [23] M.S. Siraj, S. Tasneem, D. Carlstedt, S. Duan, M. Johansen, C. Larsson, J. Xu, F. Liu, F. Edgren, L.E. Asp, *Adv Ener Sust Res* **n.d.**, *n/a*, 2300109.
- [24] J. Xu, C. Creighton, M. Johansen, F. Liu, S. Duan, D. Carlstedt, P. Mota-Santiago, P. Lynch, L.E. Asp, *Carbon* **2023**, *209*, 117982.
- [25] R. Tavano, J. Xu, C. Creighton, F. Liu, B. Dharmasiri, L.C. Henderson, L.E. Asp, *Batteries & Supercaps* **n.d.**, *n/a*, e202400110.
- [26] A. Gibaud, S. Hazra, *Curr Sci* **2000**, *78*, 1467.
- [27] S. Nunna, M. Naebe, N. Hameed, C. Creighton, S. Naghashian, M.J. Jennings, S. Atkiss, M. Setty, B.L. Fox, *Polym Degrad Stab* **2016**, *125*, 105.
- [28] D.D. Le Pevelen, in *Encyclopedia of Spectroscopy and Spectrometry (Second Edition)* (Ed: J.C. Lindon), Academic Press, Oxford **2010**, 2559.
- [29] F. Liu, H. Wang, L. Xue, L. Fan, Z. Zhu, *J Mater Sci* **2008**, *43*, 4316.